

Performance of Gas Mapping LiDAR™ for Quantification of Very High Methane Emission Rates

1. Abstract

We present single-blind test results for quantification of very high emission rates using Bridger Photonics, Inc.'s (Bridger's) airborne Gas Mapping LiDAR™ (GML) technology. Flow meter measurements from a controlled release are compared with emission rate quantification estimates from GML to determine Bridger's measurement bias and uncertainty. Wind data, a useful external input to Bridger's computation, is provided by four different sources for comparison: two on-site anemometers and two model based remote wind services. The fitted slope errors for the GML-estimated emission rates versus the ground-measured emission rates varied from 3% to 13%, for the different sources of wind data, compared to the ideal 1:1 parity ratio.

The value and importance of measuring multiple emitters (or a single emitter multiple times) to reduce the measurement uncertainty for aggregate emissions inventories is also described. The aggregate emissions based on GML measurements were within 4% of that based on ground measurements for all wind data and for the full 70-emitter data set. However, counter-balancing emission-rate-dependent biases may make these aggregate emissions errors artificially low as described herein.

2. Introduction and Motivation

Remotely quantifying the emissions rate of methane gas (the primary constituent in natural gas) is becoming increasingly important across the oil and gas industry. Accurate regional/basin-scale aggregate emissions rates are critical as inputs to predictive climate models and for grounding federal and state/provincial policy regarding emissions reduction targets and regulations. Many companies in the oil and gas industry have set voluntary methane emissions reduction goals and some have even tied executive compensation to the achievement of those goals. European natural gas customers are providing strong incentives to ensure that the methane they purchase has resulted in minimal emissions throughout the entire natural gas supply chain (i.e. production, transmission, and distribution). The United Nations Environmental Programme's (UNEP's) Oil and Gas Methane Partnership (OGMP) 2.0[1], which is being adopted broadly across the industry, includes quantification requirements moving forward. The US Environmental Protection Agency (EPA) is considering an alternate means of emissions limitation (AMEL) for regulatory[2] compliance that includes prioritization of methane leak repairs based on (coarse) emissions rate tiers to optimize emissions reduction. All of these applications require quantification of emission rates.

To address these emerging applications, Bridger set out to assess the methane emissions rate quantification capabilities of GML technology, specifically for very high emissions rates. The

ability of GML to detect and quantify emission rates has been validated many times, including a fully blind assessment by Carleton University, during which Bridger was unaware the testing was being performed[3]. During the Carleton testing, Matt Johnson's group found GML to exhibit an aggregate measurement bias of -8% and single-measurement standard deviation (1-σ) of ±31% (using on-site wind data) relative to the ground truth emission rates measured with flow meters. The Johnson group testing was performed under challenging conditions including small emission rates near and below the detection limit of GML (2.8 kg CH4/hr with 95% probability of detection for the production sector). Alternatively, studies at the high end of the range of emissions rates (>30 kg CH4/hr) have been challenging to perform because the controlled high emissions rates can cause the released methane gas to condense into liquid form or even freeze the controlled emissions components (piping, valves, flow meters, etc.), which can corrupt the measurements.

Since a single very large emitter may constitute a reasonable fraction of an aggregate emission or inventory, it is important that the accuracy with which very high emission rates can be quantified by GML is well understood. A large quantification error on such a large emitter can lead to relatively high uncertainty in the aggregate inventory and thus must be considered in developing a plan for achieving the emissions reduction goal for a particular application. For smaller emitters, which tend to be more numerous, the random measurement errors tend to average out and thus drive down the uncertainty in the aggregate inventory. To get similar averaging for statistically infrequent very large emitters it may be desired to repeat the measurement multiple times to reduce the random error and thereby approach the measurement bias.

To ensure that emissions inventories are accurate, and to enable the development of effective emissions reduction plans, this white paper is devoted to the first assessment of GML's quantification capabilities for very high emissions rates.

3. Brief Technology Background

Bridger's GML technology uses the absorption of laser light to detect, localize, and quantify methane gas. GML scans an eye-safe laser beam across the ground from an aircraft to produce path-integrated concentration imagery. Bridger also acquires digital aerial photography and topographical LiDAR, which they use to attribute the emissions to particular equipment and to accurately determine the distance between the sensor and the ground for their internal processing. All of the acquired data is geo-registered to a common global coordinate system. Bridger uses proprietary processing techniques that incorporate lateral and vertical gas concentration profiles with vertically varying wind speed profiles and other parameters for emission rate quantification. Bridger's stated detection sensitivity depends on the industry sector, but ranges from 0.47 kg CH4/hr (25 scfh) with a 95% probability of detection (PoD) in the distribution sector for utility companies (assuming unobstructed view), to 2.8 kg CH4/hr (150 scfh) with a 95% PoD for the production sector. Bridger's second-generation sensor, which is in prototype stage at the time of this white paper release, will further improve upon the detection sensitivity capabilities of GML when needed.

4. Description of Experiment and Setup

To overcome the challenges of gas condensation during controlled releases with high emission rates (> 30 kg CH4/hr), Bridger leased a commercial mobile trailer equipped with 900 kg of high-pressure methane gas (95% purity) as shown in Figure 1(left and center). This equipment is typically used for temporarily supplementing natural gas distribution supplies in municipalities when needed (e.g. pipeline repair). For the current project, the cylinders were configured to allow flow rates of up to 565 kg CH4/hr (30,000 scfh). The flow rate was controlled by adjusting a master valve that received the output from the combined cylinders. A heat exchanger was included as part of the commercial set up to prevent gas condensation that normally complicates tests at high rates. The combined flow rate was measured using an integrated flow meter (Sierra Instruments QuadraTherm 640i) which has a manufacturer-stated uncertainty[4] of ±0.75% of the reading with an additional ±0.5% of the full scale reading at lower rates (less than half the full rate). This corresponds to ±4-9 kg CH4/hr (~200-450 scfh) for the rates in this experiment. To avoid the large uncertainty this leads to at lower rates, Bridger focused this study on leak rates >100 kg CH4/hr limiting the potential ground measurement error to <10%. GML performance verification at lower rates would require a mass flow controller optimized for that range and has been already validated elsewhere.

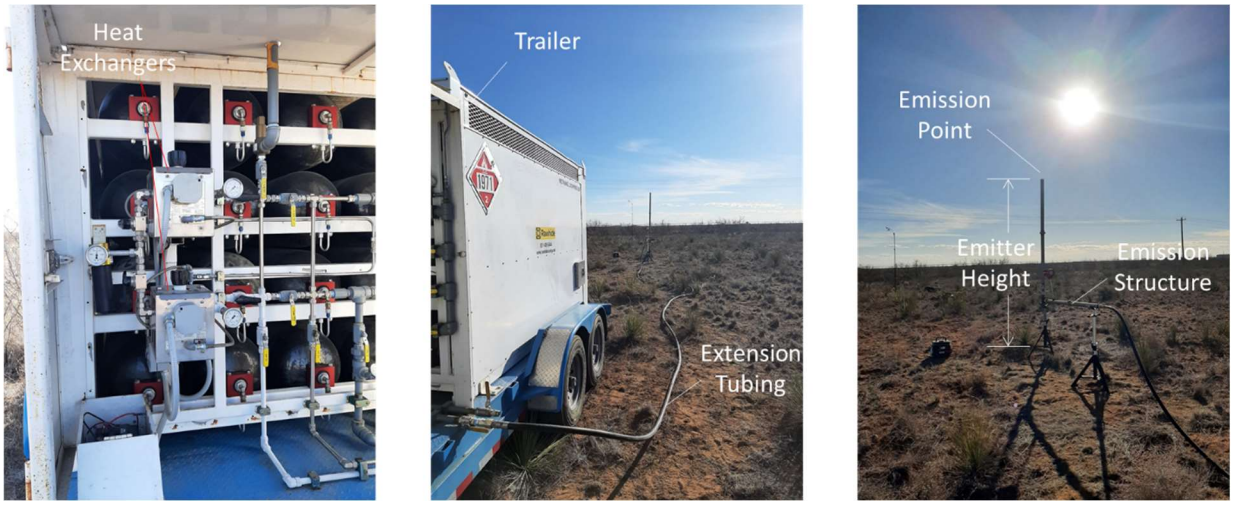

Figure 1. Left and center: Trailer equipped with a bank of high-pressure methane tanks for high emissions rates (>30 kg CH4/hr) with integrate heat exchangers to prevent freezing of the equipment. Center and right: Tubing and vertical emission structure.

During the controlled release testing, an aircraft equipped with a GML sensor flew in figure-eight patterns over the emission point and data was acquired using Bridger's standard operational protocol. Bridger used their standard flight operational conditions for the production sector which include a single-engine fixed-wing aircraft with a flight altitude between 150 meters and 230 meters above ground level (AGL) and a typical flight speed of 160 km/hr (100 mph). On the ground, tubing was used to route the gas from the trailer to the emission point located 3.5 meters vertically off the ground, as shown in Figure 1(center and right). Bridger personnel used the master valve to control the emission rate for four different nominal flow rates between 94 kg CH4/hr (5,000 scfh) and 566 kg CH4/hr (30,000 scfh). These emission rates are far greater than Bridger's minimum detection sensitivity (see above). Fifteen to twenty flight passes were performed for each emission rate for a total of 70 measurements. Experiments took place outside of Midland, Texas during two consecutive days in March 2021. All releases were properly permitted.

The local wind speed can be an important input to Bridger's emission rate quantification. To investigate the reliance on this input the wind speed was determined using several techniques during the experiment: two ground-based anemometers at the measurement site and data from two model-based remote wind services. At the emission site Bridger deployed a standard cup anemometer[5] and an ultrasonic anemometer[6] each recording wind speed and direction every second, 3 m off the ground. Additionally, Bridger accessed hourly interpolated wind speed data from Meteoblue[7] and NOAA HRRR[8]. The wind speed measured by the ultrasonic instrument varied during the testing between 5 m/s and 11 m/s, which is typical for the region.

The GML sensor data was processed using Bridger's standard operating procedures with each source of wind data to estimate each emission rate without knowledge of the actual controlled emission rates on the ground (i.e. single-blind). No additional adjustments or calibrations were made to the GML sensor beyond Bridger's standard calibration and quality assurance procedures performed before testing. In practice, Bridger uses its acquired data and computation algorithms to actively determine the height of the emitter and the spatial profile of the gas plume to minimize uncertainty in applying vertical wind profiles. For this work, the emitter height was known, which can reduce a source of uncertainty for the determination of emission rate, though Bridger's algorithms were used to compute the vertical distribution of the gas plume independently using their standard procedure.

While Bridger's processing is designed to handle multiple emission sources, background emissions, and regions of turbulent flow, none of these complications were present here. The emission rates were far above GML's detection threshold, there was only a single emitter with no interfering emissions, and the emitter was located away from obstructions. Nevertheless, these measurement conditions are routinely met throughout the Permian basin in Bridger's experience.

5. Description of Results

Results of the blind controlled release testing are shown in Figure 2 when using the MeteoBlue (top left), NOAA HRRR (top right), wind cup (bottom left), and ultrasonic (bottom right) wind data in the processing for determining emission rates from identical sets of GML data. Each light blue data point in the figures represents a single GML-measured emission rate estimate for a flight pass, while the darker blue diamonds represent the average value for each nominal emission rate, both shown as functions of ground-measured emission rate (assumed "truth"). Horizontal error bars denote errors from the mass flow controller (see above). The uncertainty of the wind measurements (not available for MeteoBlue or HRRR) are used to estimate the uncertainty of each individual measurement, while the averaged data uncertainty (vertical dark blue bars) is the standard deviation applied to the mean[9] ($\sigma/\sqrt{n}$) assuming stochastic noise. A linear fit to the complete single-measurement dataset (red line) shows strong agreement with the 1:1 parity line (green line). Deviations between the red fit line and the green parity line can represent the bias of the experiment as a function of the emission rate size. The bias is likely dominated by the uncertainty of the ground measurement at lower rates and the GML's systematic bias at higher rates.

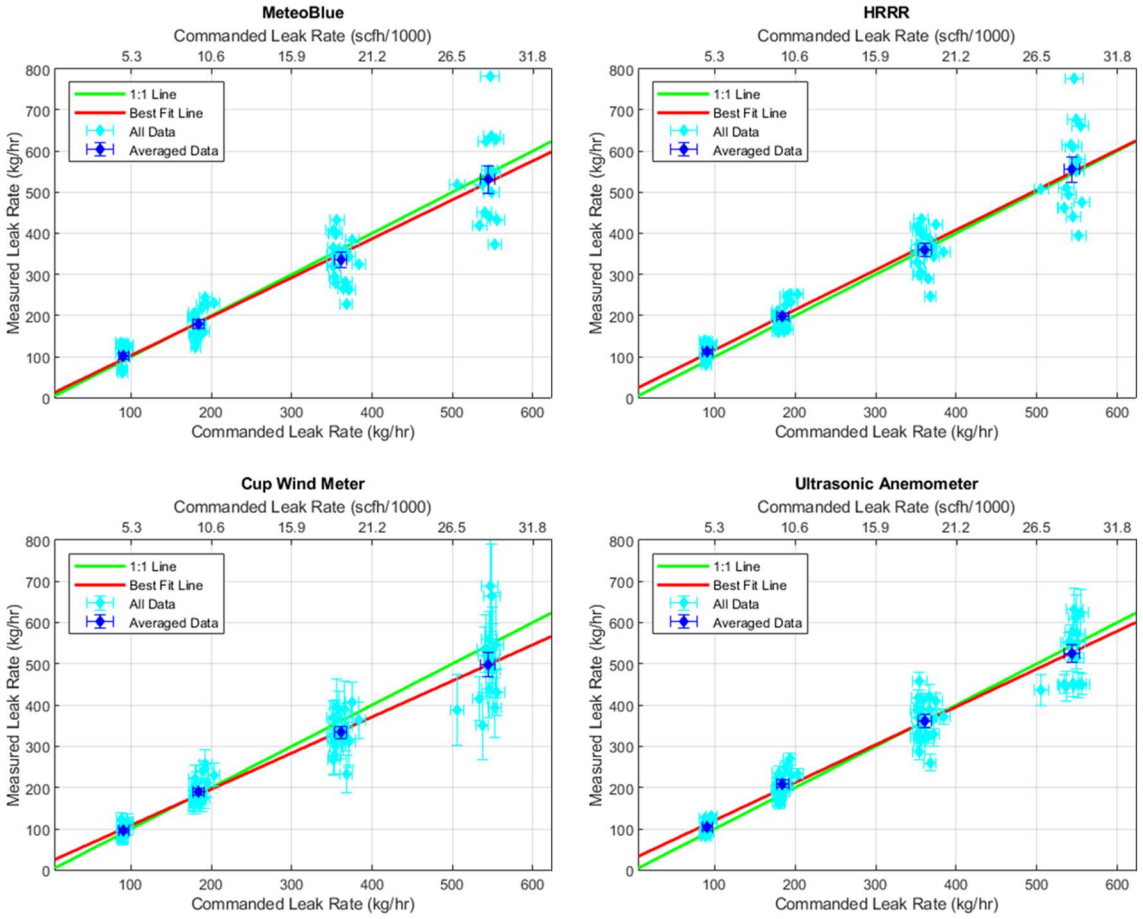

Figure 2. GML-measured emission rate versus ground-measured emission rate for four different sources of wind data: MeteoBlue (top left), NOAA HRRR (top right), cup wind meter (bottom left), and ultrasonic anemometer (bottom right). The green line represents the "ideal" 1:1 ratio and the red line is a linear fit to the data. Horizontal error bars denote errors specified for the flow meter. Vertical error bars on light blue data points are from the wind uncertainty and on the dark blue points are standard deviations of the mean.

Statistics from the fit line are shown in Figure 3. The high R^2 parameters (~0.9) for all data sets indicate high correlation between the fits and the measurements. All fit lines show slopes near the ideal value of 1, demonstrating GML's ability to accurately track methane leaks across a wide range of emissions rates with low levels of systematic bias. The fits give offsets of 8 to 29 kg CH4/hr, which, compared to the measured rates of 100's of kg CH4/hr, are relatively small, and are anticipated to be reduced with data at lower emission rates. However, due to the large errors at low flow rates of the flow meter used in this experiment and the focus on larger emissions rates, this offset is not critically measured here. The GML results compare favorably to the results from a recent study of a passive methane sensing system (solar infrared spectrometer)[10] which reports fitted slopes in the 0.88-1.45 range and R^2 values of 0.67-0.84. Solar infrared spectrometers are challenged with a variety of random and systematic effects that depend on environmental variables and conditions of the measurement scene which make it difficult to significantly and reliably reduce that technology's measurement bias[11–13]. GML's active (i.e. laser-based) methane measurement technique, on the other hand, has low sensitivity to environmental variables and measurement scene conditions, which allows for low bias and low-uncertainty measurements.

	MeteoBlue	HRRR	Wind Cup	Ultrasonic
R^2	0.87	0.89	0.89	0.92
Fit Slope	0.95 ± 0.04	0.97 ± 0.03	0.87 ± 0.02	0.92 ± 0.03
Fit Offset (kg/hr)	8 ± 13	20 ± 10	21 ± 6	29 ± 10
1-σ	21%	16%	15%	15%

Figure 3. Summary of linear fits to measured data sets computed from the four different sources of wind data, including the least squares coefficient of determination (R^2), fitted slope, y-offset, and single measurement 1-σ deviation (standard deviation).

Figure 3 also highlights the quality of the individually measured data. The single measurement uncertainty is in the 15-21% range (1-σ standard deviation), depending on the wind source, but these uncertainties consistently average to a mean value that approaches the measurement bias. The fractional spread in results can be seen below in Figure 4 which plots the percent error between Bridger's GML results and the ground "truth." The deviations of the individual data points (light blue diamonds) average down to results (dark blue diamonds) mostly within +/- 10% of the ground measured rate. Additionally, the uncertainty on these averaged results (dark blue vertical error bars) is typically within several percent due to increased measurements on the standard deviation of the mean ($\sigma/\sqrt{n}$). This illustrates that with only a relatively few independent measurements the uncertainty of an aggregate inventory can be reduced well below the single measurement uncertainty listed in Figure 3.

Figure 4 also includes the uncertainty of the ground-measured emission rate (green shaded region). This uncertainty in the "truth" grows unacceptably large at lower emission rates (e.g. +/- 20% uncertainty in the "truth" for leak rates around 30 kg CH4/hr) which is the reason smaller emission values were not studied in this experiment. Even at the lowest rate measured here the uncertainty in the ground measurement is nearly 10%. However, the fact that the bounds on most of the averaged data points (dark blue diamonds) include the "truth" uncertainty region is indicative of Bridger's ability to consistently measure large methane leaks with biases of under 10 percent.

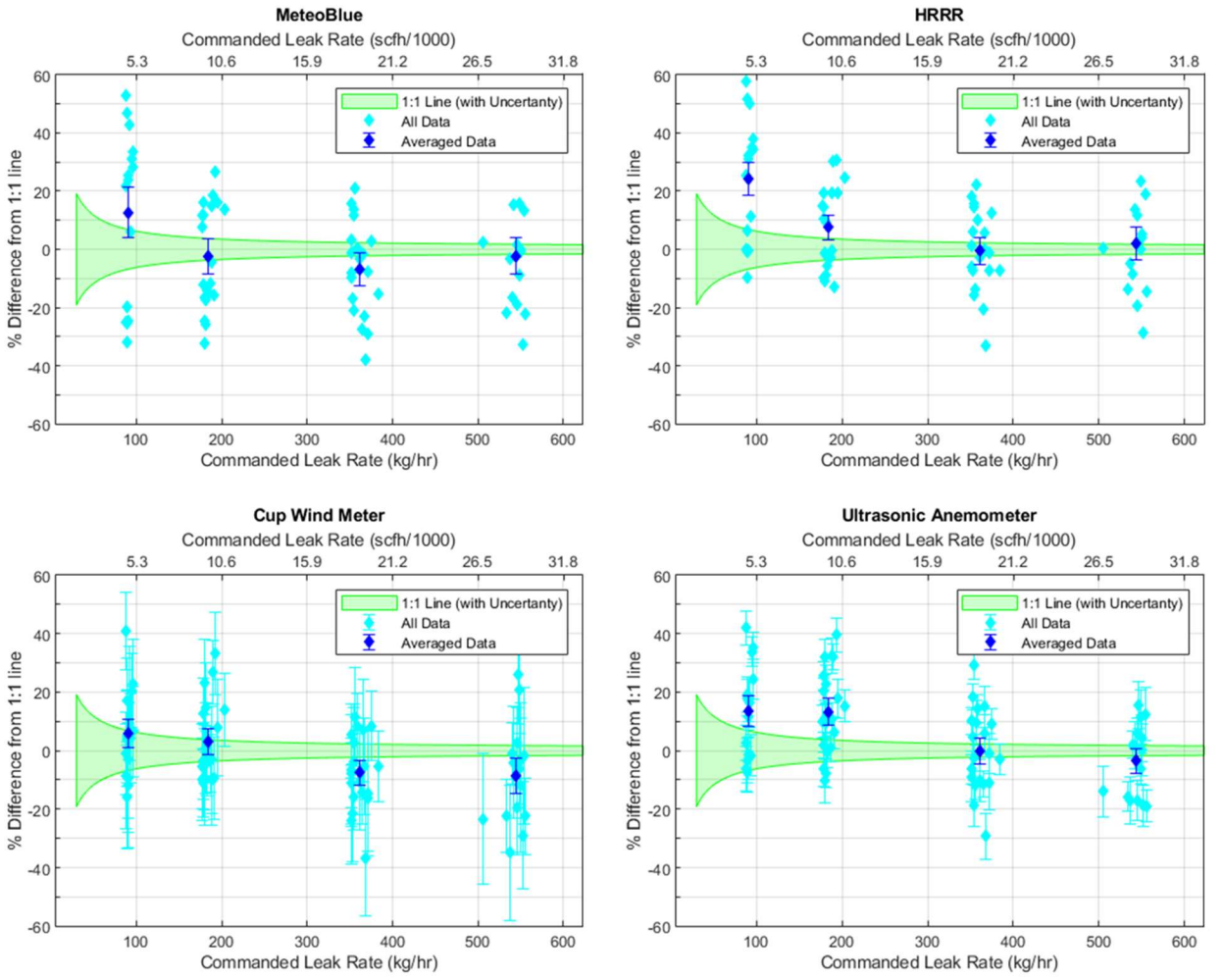

Figure 4. GML-measured emission rate deviation (in percent) from ground-measured emission rate for four different sources of wind data: MeteoBlue (top left), NOAA HRRR (top right), cup wind meter (bottom left), and ultrasonic anemometer (bottom right). The green shading represents the "ideal" zero deviation with the addition of the flow meter uncertainty which demonstrate the growing error at low emission rates. Vertical error bars on light blue (individual measurement) data points are from the wind uncertainty and on the dark blue (averaged) data points are standard deviations of the mean.

Under these experimental conditions and geographic region, the modeled and on-site wind data both yield highly accurate results, which indicates that the use of modeled wind data is an acceptable alternative for quantifying emission rates when on-site wind data is unavailable. In other geographic regions with less favorable topographic or environmental conditions, results from anemometer and model-based remote wind service data may not agree as closely.

6. Example Calculation of Aggregate Inventory Bias

The full data set measured here (70 measurements) can be used to simulate an inventory of independent emitters in order to demonstrate how the measurement uncertainty of an aggregate inventory is reduced by measuring more emitters.

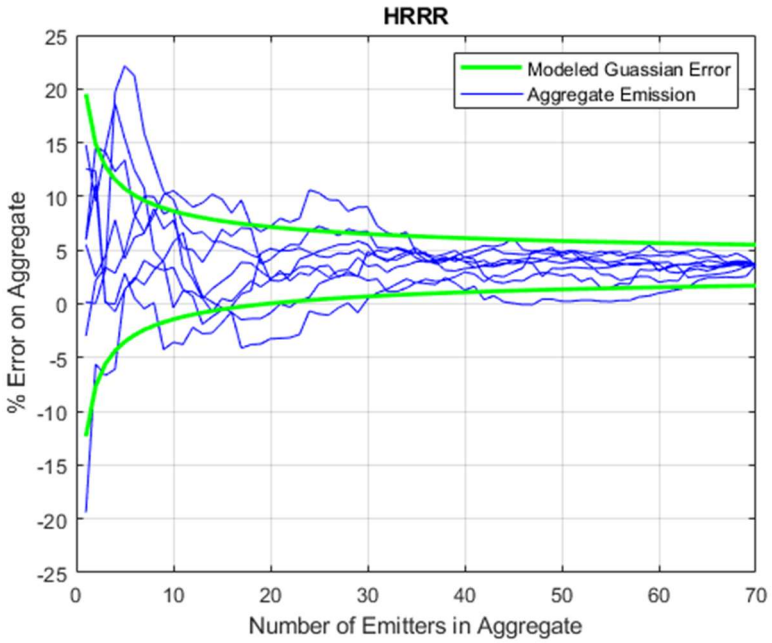

Figure 5. Example of averaging effect on an aggregate inventory. Data from the experiment (using the HRRR wind data) is randomly combined into inventories of different sizes and the error of their GML measured cumulative emission is plotted against number of emitters (blue lines). Green lines denote the $1/\sqrt{n}$ reduction of the aggregate uncertainty from the measured single emitter uncertainty (from Figure 3). This specific dataset results in a final bias of <4% from the ground measurements as seen in the convergence of the traces on the right.

Figure 5 shows the percent error of the aggregated emission rate (i.e. the percent error of the simulated inventory) as a function of the number of emitters included in the aggregate, up to the total of all 70 emitters. Each blue line represents a different order (randomly selected) in which the emitters are "measured" for the inventory (using the HRRR wind data). When including only a few emitters in the aggregate (left side of plot) the spread in the aggregate error is comparatively large, but as more emitters are added in their cumulative uncertainty is greatly reduced. With a large number of measurements (right side of plot) the traces converge to a non-zero value, which is the measurement bias of this inventory (<4% for the HRRR wind data shown here). All blue traces are identical at N=70 emitters because all the measured data is included.

The green traces in Figure 5 are $\pm\sigma/\sqrt{n}$ (where σ is the single measurement uncertainty from Figure 3) offset by the bias. The blue traces are well bounded by these lines indicating that each individual measurement has gaussian-distributed noise with its well-understood averaging behavior. It is useful to note that the largest reduction in aggregate uncertainty occurs in the first ~10 measurements, demonstrating that an inventory consisting of a relatively small number of emissions may achieve sufficient accuracy for a given application. Additional measurements beyond ~10 may provide only marginal reductions in the uncertainty.

The results in Figure 5 are meant to be illustrative of the benefits of aggregating an inventory. The <4% aggregate bias presented here, which was observed for all sources of wind data, may be favorably impacted by several factors. First, the bias of an individual GML measurement is a function of the emission rate. Figure 4 shows that measurements of lower emission rates are typically skewed positive (generally positively biased) which is very likely due to errors in the flow meter. Whereas measurements of higher emission rates are typically skewed slightly negative, which may be due to bias in the GML measurement. Since the measured emission rates are fairly

uniformly distributed, these two systematic effects effectively balance one another, which may result in an unrealistically small aggregate bias. A different distribution of emission rates may therefore result in a different bias on the aggregate. Additionally, without the counterbalancing bias of the flow meter, the less than unity measurement slopes may add up to larger aggregate biases. Second, Bridger has not yet comprehensively studied if the GML measurement bias may vary between factory calibrations. This could compound systematic errors from different measurements and reduce the ability to average down the aggregate measurement uncertainty. Finally, biases in the input wind data will translate into biases in the GML measurements. The Permian basin, being largely flat, unobstructed, and with a relatively dense network or weather station, has fairly reliable wind data from model-based remote wind services (such as MeteoBlue and HRRR). This can be more complicated in other regions leading to unknown systematics in the determination of emission rates when using remote wind service data.

Despite these caveats the GML emissions rate quantification results shown here indicate strong potential to accurately quantify large leak rates under these realistic measurement conditions. By measuring many emitters in an inventory, the measurement uncertainty can be reduced well below the single-measurement uncertainty.

7. Conclusions

This white paper presented blind emission rate quantification testing of Bridger's GML technology. Data analyzed using Bridger's standard algorithms showed strong agreement with the ground-measured leak rates using both locally-measured and regionally-interpolated wind data inputs. The deviations of the fitted slopes from the ideal 1:1 slope ranged from 3% to 13% depending on the wind data source. Moreover, the aggregate measurement bias for large emission rates (100-550 kg CH4/hr) was shown to be single digit percent. This result highlights the ability to significantly reduce uncertainty, and approach the measurement bias, in aggregate emissions measurements (e.g. inventories) by measuring multiple emitters.

Acknowledgments

Bridger gratefully acknowledges the suggestion and information provided by Dr. Adam Brandt and Dr. Evan Sherwin, both of Stanford University, regarding the high emission trailer setup used for this work. Also, Bridger has learned and gratefully acknowledges that the high emissions trailer setup was originally assembled and made possible by previous efforts funded by Stanford University and the Environmental Defense Fund. The engineering work that went into the trailer setup was critical to performing Bridger's study.

Contact: Info at 406.522.3766 or info@bridgerphotonics.com

Bibliography

1. https://www.ccacoalition.org/en/resources/oil-and-gas-methane-partnership-ogmp-20-framework.
2. EPA 40 CFR Part 60, https://www.govinfo.gov/content/pkg/FR-2016-06-03/pdf/2016-11971.pdf, accessed 5/26/2021.
3. Johnson, M. R., Tyner, D. R. & Szekeres, A. J. Blinded evaluation of airborne methane

source detection using Bridger Photonics LiDAR. *Remote Sens. Environ.* **259**, 112418 (2021).
4. https://www.sierrainstruments.com/products/quadratherm/640i.html.
5. https://www.onsetcomp.com/products/sensors/s-wcf-m003.
6. https://lcjcapteurs.com/en/girouette-anemometres-capteur-vent/sa-dzp-2/.
7. https://www.meteoblue.com/.
8. https://rapidrefresh.noaa.gov/hrrr/.
9. NIST/SEMATECH e-Handbook of Statistical Methods, http://www.itl.nist.gov/div898/handbook/, accesssed 5/26/2021.
10. Sherwin, E. D., Chen, Y., Ravikumar, A. P. & Brandt, A. R. Single-blind test of airplane-based hyperspectral methane detection via controlled releases. *Elementa* **9**, (2021).
11. Ayasse, A. K. *et al.* Evaluating the effects of surface properties on methane retrievals using a synthetic airborne visible/infrared imaging spectrometer next generation (AVIRIS-NG) image. *Remote Sens. Environ.* **215**, 386–397 (2018).
12. Thorpe, A. K. *et al.* Mapping methane concentrations from a controlled release experiment using the next generation airborne visible/infrared imaging spectrometer (AVIRIS-NG). *Remote Sens. Environ.* **179**, 104–115 (2016).
13. Minwei, Z., Leifer, I. & Hu, C. Challenges in Methane Column Retrievals from AVIRIS-NG Imagery over Spectrally Cluttered Surfaces: A Sensitivity Analysis. *Remonte Sens.* **9**, 1–21 (2017).